

ALMA MEMO 333
52 YEARS OF CLIMATOLOGICAL DATA FOR THE
CHAJNANTOR AREA

Ricardo Bustos

Avda. Francesa 292, Concepción, Chile

Email: rbustos@dgf.uchile.cl

Guillermo Delgado

Onsala Space Observatory / European Southern Observatory

Casilla 19001, Santiago 19, Chile

Email: gdelgado@eso.org

Lars-Åke Nyman

Onsala Space Observatory / European Southern Observatory

Casilla 19001, Santiago 19, Chile

Email: lnyman@eso.org

Simon Radford

National Radio Astronomy Observatory

949 North Cherry Avenue Tucson, AZ 85721-0655, USA

Email: sradford@nrao.edu

Abstract – We present 52 years of weather data for the Chajnantor area. This data has been prepared by the National Center for Environmental Prediction (NCEP) and the National Center for Atmospheric Research (NCAR) from historical weather observations and state of the art climatological models. The basic idea of the NCEP/NCAR reanalysis project is to provide reliable historical weather data from 1948 to the present. The data is referenced to a $2.5^\circ \times 2.5^\circ$ global grid. One of these grid points is located in Salar de Chalviri (Bolivia), about 60 km to the north of Chajnantor at a height of approximately 4,000 m.

The reanalysis data produced for this grid point are estimated from radiosondes, weather stations, satellites, and other sources scattered in a large area including Chile, Peru, Bolivia and Argentina. In order to find out if this data can be used to study the long term weather pattern on Chajnantor, at a height of 5,050 m and 60 km away, we compared 5 years of ground temperature and precipitable water vapour (*PWV*) measured at Chajnantor between 1995 and 2000. The *PWV* at Chajnantor is calculated from opacity measurements by a 225 GHz tipping radiometer.

The comparison of the NCEP/NCAR reanalysis data corrected for the altitude of Chajnantor and the actual data measured during the last five years is very good. We therefore believe that the reanalysis data can be used to study the long-term climatological variations on Chajnantor.

The data presented for the 52-year period shows that the Chajnantor area is indeed a place with very low *PWV* contents, with clear seasonal indications of higher humidity during the austral summer. Climatological cycles can be seen, but the 52 years of data show that anomalies larger than the ones that we have experienced during the last years are not to be expected.

1 Introduction

Chajnantor, the selected site for the construction of ALMA, has been monitored since 1995 by NRAO and since 1998 by ESO. From the initial observations, it was concluded that Chajnantor is an excellent site for millimetre and submillimetre astronomy, showing some of the best 225 GHz transparencies ever measured, comparable only with those measured at the South Pole [1]. The collected data during the last years has shown that the weather does not always follow the excellent conditions observed during the first years of site testing. During the last years we have experienced severe altiplanic summer storms and the question about a global trend on the Chajnantor area becomes relevant, but the collected data is not enough for a serious statistical analysis.

Some alternatives for long term studies do exist, for example at the near town of Calama (160 km, north-west of Chajnantor), weather data has been gathered since 1960. The analysis of this data is a good alternative to access a long time series of regional data. The use of this data should be done with care since Calama is located at 2,300 m, behind the Cordillera de Domeyko, a small mountain range. Hence the weather there might not be directly related to the one at Chajnantor. Another problem with this data is that the cost to access it is still very high. Nevertheless, some negotiations are being carried out in order to obtain this data.

Satellite pictures have been proposed, but they have several disadvantages: price, resolution, and not very long historical records.

Here we use public data available in the web [2] coming from the reanalysis of all available historical data from 1948 to the present. State of the art analysis/forecast models produce atmospheric variables every 6 hours on a global scale. Comparing the output of the model with actual data, it is possible to improve the model parameters to achieve good fitting at the measured points. Finally, the output of this reanalysis is referenced to a global grid with multiple vertical levels.

The meteorological data is obtained from all available sources. This effort involves the recovery of surface land and ship weather stations, rawinsonde (radiosonde with wind measuring capability), pibal (pilot balloon), aircraft, satellite, and other data.

2 The National Center for Environmental Prediction (NCEP) and the National Center for Atmospheric Research (NCAR) reanalysis

The National Center for Environmental Prediction (NCEP) and the National Center for Atmospheric Research (NCAR) started a joint project to use all available weather data since 1948 to the present. The idea is to reanalyse this data (hence the name of NCEP/NCAR reanalysis), using a state-of-the-art analysis/forecast system and perform data assimilation using past data (reanalysis). A 6-hour forecast is first performed to later correct towards the observed values. Then, the reanalysis is done at NCEP, providing the initial conditions for the next 6-hour integration. The output reanalysis files of atmospheric variables are calculated every 6 hours on a 2.5°x2.5° global grid at 17 vertical pressure levels.

The same frozen analysis/forecast system will continue to perform data assimilation into the future so that climate researchers can assess whether current climate anomalies are significant when compared to a long reanalysis without changes in the data assimilation system.

The reanalysis gridded data fields have been classified into four classes, depending on the relative influence of the observational data and the model on the gridded variable. An A-class indicates that the analysis variable is strongly influenced by observational data, and hence it is the most reliable. B-class indicates that, although there are observational data that directly affect the value of the variable, the model also has a very strong influence on the analysis value. C-class indicates that there are no observations directly affecting the variable, so it is derived solely from the model fields. D-class represents a field that is obtained from climatological values and does not depend on the model.

A more detailed explanation of the NCEP/NCAR reanalysis project is done by Kalnay *et al.* [3]. It is enough here to say that the NCEP/NCAR reanalysis system has three major modules: Data decoder and quality control preprocessor, Data assimilation module, and Reanalysis output module.

2.1 *Data decoder and quality control pre-processor*

This is a major task performed at NCAR. Surface and upper-air observations are prepared for reanalysis reformatting the data coming from many different sources into a uniform binary representation.

The data is obtained worldwide from many international sources such as Global Telecommunication System (GTS), NOAA/National Environmental Satellite Data and Information System (NESDIS), Geophysical Fluid Dynamics Laboratory (GFDL), United Kingdom Meteorological Office (UKMO), Japanese Meteorological Agency (JMA), European Center for Medium-Range Weather Forecasts (ECMWF), among others.

The collected dataset are:

- Global rawinsonde data
- Comprehensive Ocean-Atmosphere Data Set surface marine data (COADS)
- Aircraft data
- Surface land synoptic data
- Satellite sounder data
- SSM/I (Special Sensing Microwave/Imager) surface wind speeds
- Satellite cloud drift winds.

Most of this information covers the period from about 1948 to the present, with some data not available at different locations and for different periods. For example, the rawinsonde observing networks for Antarctica and the West Coast of South America did not start until July 1957, new satellite data is becoming available throughout the years, SSM/I became available in July 1987, etc.

The method uses large datasets of observations, with new observation methods becoming available during the last years. On the question on how to handle the changes in the observation system, especially the introduction of satellite data, the reanalysis uses all the available data at a given time instead of selecting a subset of the observations that can remain stable throughout the period of reanalysis. This yields to an analysis that is as accurate as possible throughout the 52-year reanalysis.

At this stage major data problems are detected, such as wrong dates, wrong locations, satellite data with wrong longitudes, garbled information, etc. The preparation of the surface boundary conditions is done here.

The data is later quality controlled, cross-checking the observations with software modules and human operators, searching for statistical anomalies.

2.2 *Data assimilation module*

This is the central part of the NCEP/NCAR reanalysis. Here is where the data is assimilated to the output of global weather models and a new stage of quality control is performed.

Archiving is done here, saving the original observations together with processing information. In addition, periodic forecast are done serving as indirect estimates of the accuracy of the analysis.

2.3 *Reanalysis output module*

The reanalysis output module includes several different archives:

- Binary Universal Format Representation (BUFR) observational archive with the original data.
- Main synoptic archive: Contains a large number of analysis and first-guess fields at 00:00, 06:00, 12:00, and 18:00 UTC on a 2.5°x2.5° grid. It also contains some statistical variables obtained during the fitting.
- Reduced “time series” archive: This archive contains basic upper-air parameters at standard pressure levels saved in GRIB format readable with the Grid Analysis and Display System software (GrADS). The 17 pressure levels are 1000, 925, 850, 700, 600, 500, 400, 300, 250, 200, 150, 100, 70, 50, 30, 20, and 10 mbar. Data fields are saved on a 2.5°x2.5° grid. It contains data from 1948 onwards, four times per day at 00:00, 06:00, 12:00, and 18:00 UTC, daily and monthly averages and long-term means.
- Quick-look CD-ROM: Database that fit in a small (1 per year) number of CD-ROMs.
- Automatic monitoring system for the reanalysis output: At the end of each month of reanalysis, time series at all standard pressure levels are compared with climatological models and statistical variables are calculated.

3 Meteorology data available for the Chajnantor area

3.1 *NCEP/NCAR reanalysis*

In the Chajnantor area, the data collection used by the NCEP/NCAR reanalysis includes several Chilean ground stations and rawinsonde data. The closest Chilean ground station to the area is Calama/El Loa (22.50° S, 68.90° W, 2,320 m). Antofagasta/Cerro Moreno (23.43° S, 70.45° W, 140 m) station obtains rawinsonde data every day at 00:00 and 12:00 UTC. Surface observations are also done at this station.

The map in Figure 1 shows the 49 ground stations in Peru, Bolivia, Chile, and Argentina near the Chajnantor area (green dots). The availability of each station is not always permanent and depends on human factors to send the data correctly to NCAR or to other appropriate organisation. Extra data can

be obtained from different temporary ground stations or by rawinsonde experiments. A complete world-wide list can be found in [4].

In this work, we use the NCEP/NCAR reanalysis data at the closest grid point to Chajnantor. This grid point is located in the south west of Bolivia at Salar de Chalviri (22.5° S, 67.5° W), about 60 km. north from Chajnantor (23.02° S, 67.75° W). It corresponds to a site at a surface geopotential height (D-class variable) of 4,029 m according to the NCEP/NCAR reanalysis, but its real altitude might be closer to 4,400 m according to maps of the area. As first estimation absolute surface values for this grid point do not correspond to absolute values for the Chajnantor site at 5,050 m. However, variations, tendencies, and anomalies of these values can be considered similar at both sites. To compare magnitudes, a correction must be introduced to compensate for the height difference between the two sites.

The selected time series for this work are monthly averages for temperature, pressure, and precipitable water vapour (*PWV*) at the surface. Other meteorological variables can be obtained and also at different pressure levels. Some of these have been presented before in [5]

3.1.1 *PWV*

NCEP/NCAR precipitable water data is a B-class variable, partially defined by observations but strongly influenced by the model characteristics [3, 6].

Due to the NCEP/NCAR model characteristics, very low *PWV* values can appear as negative values. These negative values do not have any physical meaning. Here we discarded the negative values.

Considering that the NCEP/NCAR reanalysis is giving the *PWV* for a grid point at 4,029 m and the Chajnantor site is at 5,050 m, we need to correct the *PWV* for the height difference. Here we will only correct for this height difference and will not consider any other difference based on the geographical location of both points.

If water vapour density is exponentially distributed in altitude [7], we have:

$$\rho(h) = \rho_0 e^{-h/h_0} \quad (1)$$

with ρ_0 the water vapour density at the ground (reference level), and h_0 the scale height factor for this distribution, considered to be about 1,500 m for Chajnantor [8].

PWV is obtained by integrating $\rho(h)$ over the entire atmospheric column from ground to an altitude h :

$$PWV = \int_0^h \rho_0 e^{-h/h_0} dh = \rho_0 h_0 (1 - e^{-h/h_0}) \quad (2)$$

when h is sufficiently large:

$$PWV \approx \rho_0 h_0 \quad (3)$$

The NCEP/NCAR data used here gives the value of *PWV* at a point at 4,029 m, thus we can estimate the water vapour density at this surface by:

$$\rho_0 = \frac{PWV_{4029}}{h_0} \quad (4)$$

Considering an altitude of 5,050 m for Chajnantor and using equation (1) and (4), then the water vapour density at 5,050 m, 1,021 m above the grid point, will be given by

$$\rho(5050) = \frac{PWV_{4029}}{h_0} e^{-1021/h_0} \quad (5)$$

Replacing $\rho(5050)$ in equation (3), the *PWV* at 5,050 m can be calculated as:

$$PWV_{5050} = PWV_{4029} e^{-1021/h_0} \quad (6)$$

Replacing $h_0 = 1,500$ m into equation (6) we obtain

$$PWV_{5050} = 0.5063 PWV_{4029} \quad (7)$$

From equation (7) we have that the PWV data from NCEP/NCAR reanalysis has to be multiplied by an altitude correction factor of 0.5063 in order to compare it with PWV measured at Chajnantor.

3.1.2 Temperature

NCEP/NCAR surface temperature data is considered as an A-class variable when given at the different pressure levels, but it is considered a B-class variable at surface, partially defined by observations but strongly influenced by the model characteristics [6]. This data should also be corrected for the altitude difference between the two points.

The temperature of a dry air parcel decreases with altitude at the *dry adiabatic lapse rate* $\Gamma_d = 9.8$ °C/Km. Under saturated conditions, the temperature of this parcel decreases at the *saturated adiabatic lapse rate* $\Gamma_s \cong 6.5$ °C/Km [9]. From radiosonde measurements at Chajnantor, variable lapse rates are found between 7 and 9.3 °C/Km. Different mixing ratio due to dynamical processes such as solar radiation and wind can produce different lapse rate near the surface depending on the time of the day and year. If we consider an average lapse rate for Chajnantor of 8 °C/Km, the average temperature difference between the grid point and Chajnantor should be 8.17 °C.

Calculating the NCEP/NCAR average temperature and the Chajnantor ground station average temperature for the complete 5-year period, a 6.4 °C difference is obtained. The 1.77 °C difference with the theoretical value can be attributed to an overestimation of the NCEP/NCAR surface temperature or due to the approximated value of 8 °C/Km estimated for the Chajnantor lapse rate. The result agrees for a saturated air parcel, which is not the case at Chajnantor. In order to compare the datasets, 6.4 °C have been subtracted from the NCEP/NCAR temperature data.

3.1.3 Pressure

For the case of pressure, we assume an exponential decay with a scale height H according to Houghton [10], given by:

$$P(h) = P_0 e^{-\int_0^h \frac{1}{H(h)} dh} \quad (9)$$

$$H(h) = \frac{RT(h)}{M_d g} \quad (10)$$

Where P_0 is the pressure at ground level [mbar], R is the molar gas constant, M_d is the molecular weight of “dry” air, and g the gravitational constant. At Chajnantor, this model compared with radiosonde measurements gives an agreement within 0.5% up to 8,000 m [11].

Using an average value H_0 for the pressure scale height $H(h)$ of 7.2 km, we obtain a correction factor between the grid point data and Chajnantor of 0.8678, using a height difference of 1,021 m.

3.2 Chajnantor ground data

The weather and atmospheric data measured at Chajnantor is available on the web [12]. In order to perform a check on the reanalysis data we used temperature data and PWV data. The PWV is derived from opacity measurements done at 225 GHz.

For the ground data at Chajnantor, a one-hour average value for 00:00, 06:00, 12:00, and 18:00 UTC is considered (30 minutes before and after the time considered).

3.2.1 PWV

The 225 GHz opacity, τ , is obtained every 10 minutes approximately [13]. This value is converted to *PWV* using a relation between opacity and *PWV*. In [11] a second order polynomial was given to relate *PWV* and 225 GHz opacity based on measurements done with a 183 GHz radiometer. Here we use a linear relation obtained by the same procedure outlined in [11], but using a larger dataset.

$$PWV = -0.052088 + 20.876\tau \quad (8)$$

This empirical expression is valid for Chajnantor, a site at a height of 5,050 m.

The raw opacity data can contain errors. These errors can either be default error values represented by a -999 (0.358% of the data) or too high τ values obtained during scanning of the radiometer. Here we define as “bad” those opacity values higher than 0.5. From equation (8) we have that a value τ greater than 0.5 implies a *PWV* value greater than 10.4 mm, a value seldom seen at Chajnantor. The error values are eliminated from the analysis. Both kinds of errors take about 2.5% out of the original data.

In the interval starting on April 5 1995 to July 31 2000, 82.14% of the averaged opacity data is used. The other 17.86% are discarded values due to errors or non-existent data.

3.2.2 Temperature

The raw ground meteorological data at Chajnantor shows some relatively long periods with no data when instruments were malfunctioning. For the period April 5, 1995 to July 31, 2000, 20.47% of the averaged data is not available.

4 Reliability of the atmospheric reanalysis

Different studies [14, 15], have shown some differences between the NCEP/NCAR Reanalysis and other reanalysis data, but they do not necessarily conclude in which reanalysis system the data is more reliable. Recently, it has been noted that although the reanalysis system has remain essentially unchanged during the 52 years processed, there were two major changes in the observing system [15]. The first change took place between 1948-1957 when the upper-air network was gradually established, and the second change was in 1979 when the global use of satellite soundings was introduced. This new satellite data resulted in a significant change in the climatology, especially above the height given by 200 mb and south of latitude 50° S, suggesting that the climatology based on data from 1979 to present days is more reliable. Evaluating “recasts” at the end of the Data Assimilation Module it is possible to find that the first decade is less reliable than the last four decades.

4.1 The Visviri experiment

An important work to compare the NCEP/NCAR reanalysis data with upper-air observations in the South American Altiplano is presented in [16]. This is part of a project aimed to improve the understanding of regional climate dynamics during the wet season in the South American Altiplano.

Intensive surface and upper-air measurements (4 rawinsonde measurements per day) were carried out at Visviri (17.60° S, 69.50° W, 4,070 m) during two 10-days periods in January 1994 (Visviri I) and January 1995 (Visviri II). Soundings were performed at 09:00, 13:00, 17:00 and 21:00 hours (local time) in Visviri I, and at 09:00, 13:00, 18:00 and 24:00 hour (local time) during Visviri II. The average vertical profiles of temperature, humidity, wind and geopotential height, and the associated diurnal cycles were compared with those obtained from the NCEP/NCAR reanalysis at the closest grid point (17.50° S, 70.00° W).

The result of this comparison shows that reanalysis captures the major features in the vertical structure of these variables and also the interannual changes from a relatively wet period in Visviri I to a much drier conditions in Visviri II. Nevertheless, some discrepancies, both in the strength and timing of the

diurnal cycle and particularly in the westward transport of water vapor across the Andes, were found. These values are significantly underestimated by the reanalysis. There are also significant differences at ground level.

The results obtained in [16] are coherent with the final comments of [6] on that the NCEP/NCAR reanalysis data has proved to be particularly useful in the study of the spatial pattern of climate variability at different timescales. Daily, seasonal, and interannual variability is well captured by reanalysis, though long-term trends are not well represented specially in the southern hemisphere because of the sparse data and that the observation network started at a much later time than in most of the northern hemisphere.

Because the result was not conclusive, we cross-compare the reanalysis data with ground measured data taken at Llano de Chajnantor.

4.2 *Five year comparison with ground measured data at Chajnantor*

To have confidence in the historical data of the NCEP/NCAR reanalysis, we have to compare this data with actual data measured at Chajnantor. Site testing activities in the area have been carried out since 1995 and the almost continuous meteorological and atmospheric data obtained there is a very good source to compare with the reanalysis results [17].

4.2.1 *PWV*

The *PWV* derived from 225 GHz radiometer data is cross-compared with the NCEP/NCAR *PWV* data. In the NCEP/NCAR reanalysis *PWV* data, all negative values are eliminated, while in the 225 GHz radiometer data, all error values are eliminated. The cross-correlation of these two datasets, is done considering three subsets: four-times per day measurements, daily average, and monthly average. The correlation for the four-times per day measurements is 0.47, for the daily average is 0.57, and for the monthly average 0.79.

The compared datasets can be seen in Figure 2. The reanalysis data is previously multiplied by the altitude correction factor 0.5063 from equation (7), and the 225 GHz radiometer data is converted to *PWV* using equation (9).

The upper plot shows the *PWV* data at four times per day (00:00, 06:00, 12:00, and 18:00 UTC), the centre plot shows daily *PWV* averages, while monthly *PWV* averages are seen in the lower plot. It can be seen that the radiometer *PWV* data is well followed by reanalysis. A 0.79 cross-correlation value indicates a good correlation between the NCEP/NCAR *PWV* data and the radiometer *PWV* data. Tendencies for the *PWV* during summers from 1996 to 2000 are similar, and the signature of the winters is clearly seen. However, during part of the time the reanalysis *PWV* data does not agree on magnitude with measured *PWV* radiometer data, specially for the August 1997 to June 1998 period.

4.2.2 *Temperature*

The Chajnantor ground station temperature data are cross-correlated with the NCEP/NCAR temperature data. The cross-correlation of these two datasets, is done considering three subsets: four-times per day measurements, daily average, and monthly average. The correlation for the four-times per day measurements is 0.68, for the daily average is 0.78, and for the monthly average 0.87.

The lower graph in Figure 3 shows monthly temperature averages from 1995 to the present. It can be seen that NCEP/NCAR reanalysis temperature data follows the same trend as the temperature observed at Chajnantor. In fact, a cross-correlation value of 0.87 indicates a good reliability of the reanalysis temperature data. Maximum temperatures during summer of 1998 and 1999 have been underestimated by reanalysis, though descending tendencies of average temperatures during summer of 1998 to 2000 are captured in both cases.

5 52-year climatology for Chajnantor

Here we present 52-year time series for temperature, pressure, and *PWV* at the surface for the period 1st of January 1948 to 31st of July 2000. The temperature and *PWV* monthly averages are corrected for altitude from the value given by the NCEP/NCAR reanalysis for the grid point at Salar de Chalviri by using the correction scheme described in 3.1.1 and 3.1.2.

Coloured isopleth diagrams (annually versus monthly values) showing pressure and temperature can be seen in Figure 4, together with the anomaly plots of the monthly averages to the historical average.

The pressure plots (upper two plots in Figure 4), show clearly the signature of the altiplanic summer storms, with higher pressures during summer, even extending into fall and winter. The anomaly plot shows that from about 1976 the pressures have been higher than average.

For the case of the surface temperature, shown in the two last plots, it can be seen that there are temperatures higher than average associated with the periods of higher average pressure (1976 to 1997) and viceversa. The most striking result (already seen in section 4.2.2) is that the average temperature for the last two years is declining.

Figure 5 shows the *PWV* for Chajnantor. Here, in the two upper plots, we have isopleths for *PWV* at two resolutions, with the upper plot (0 to 6 mm) showing details for the wetter summer period. The second plot (0 to 2 mm) shows details for the dryer winter period.

The centre plot in Figure 5 shows the anomalies for *PWV* expressed as percentage. This plot shows clearly a winter cycle with higher *PWV* averages of about 8-10 years. The last cycle with winters wetter than average was during the years 1997 and 1998.

The fourth plot in Figure 5 shows the time series for anomalies for the months of January and February expressed as a percentage. From this plot we can conclude that the anomalies during the last 52 years have been within $\pm 40\%$ from the average value.

The last plot shows the anomalies for July, during austral winter. Here we see that the *PWV* varies by a factor of four around the average.

Figure 6 shows the time series for the monthly average of *PWV*. Here it is possible to distinguish a modulation of the maximum average during summer, showing the same cycle seen before.

6 Analysis and conclusions

Performing an FFT to the time series of the NCEP/NCAR *PWV* corrected for the altitude of Chajnantor (Figure 6), it is possible to obtain some cyclic components, this exercise can be done separately during summer and winter times. Variable cycles between 2 and 6 years can be observed, as well as a cycle between 10 and 11 years. These cycles seem to be in agreement with the spacing between El Niño Southern Oscillation (ENSO), a term that is used as a general name to include also the La Niña phenomenon.

ENSO is the most important ocean-atmosphere coupled phenomenon causing global climate variability on interannual time scales. According to Wolter [18], the strongest historic El Niño events since 1950 started in 1957, 1965, 1972, 1982, 1986, 1991, and 1997 with variable durations of half a year to one and a half years. The strongest La Niña events started in years 1949, 1954, 1964, 1970, 1973, 1975, 1988, and 1998 with the effects of La Niña lingering well beyond the demise of the event. The duration of these events has been compiled by the Climate Prediction Center [19]. The main difference between these two events is that during an El Niño event, the waters in the Pacific Ocean become warmer than usual, while in La Niña times, the water becomes colder. This change in water temperature triggers a series of global events affecting the local weather conditions, including those at the astronomical observatories.

From Figure 7, it is possible to relate these global climate phenomena to the winter *PWV* values at Chajnantor. On the anomaly plot, it is possible to see that wetter periods during winter usually follow an El Niño event, while wintertime dryer conditions follow a La Niña event. The dryer conditions after La Niña seems to last longer than the wetter ones after El Niño. During 1998, a La Niña episode was registered coinciding with the dryer conditions that we are experiencing according to the anomaly plots. This can also be seen in Figure 2 where the average values of *PWV* measured at Chajnantor during winter times are lower during the winter of 1999 than on the previous two years.

On the other hand, the presence of an ENSO phenomenon does not seem to be linked with the magnitude of the average value of *PWV* during the austral summer period, but rather with the extension of the “bad weather” into fall and winter (extension of the altiplanic summer storms). The variation of the maximum monthly average of *PWV* on the summer months does not vary by more than $\pm 40\%$ from the historical (52-year) average.

To resume, it is possible to say, based on 52-year historical data, that Chajnantor can experience cycles affecting chiefly the average value of *PWV* during wintertime. The extension of the more humid conditions during summer beyond the summer months needs to be studied more carefully in connection with ENSO.

From the temperature anomaly plot in Figure 4, it is possible to see that during the first 18 years (1954 to 1972) the temperatures and pressures were lower than the historical average. This is reversed in the next 22 years (1972 to 1998) when the temperature and pressure anomalies become positive. There are a few small but not significant exceptions to this general tendency. From Figure 7 it is possible to see that during the first 18 years there is a predominance of La Niña events, with a few very spaced El Niño. Whereas during the next 22 years we have more closely spaced El Niño events, with just two occurrences of La Niña. This relation between pressure and temperature with ENSO might be a useful forecast tool for the winter quality and needs to be explored more.

The data indicates that during the last two years we have experienced a La Niña episode, characterised by dryer and colder winters.

Due to the nature of the NCEP/NCAR reanalysis data, the climatological results obtained here are valid in the complete Chajnantor area, with small local differences between Chajnantor and Pampa La Bola given only by the local topography and height difference.

Acknowledgements

Special thanks are given to Dr. José Rutllant and Dr. René Garreaud for their useful comments, access to documentation and for the authorisation to use the facilities at the Meteorology Section of the Department of Geophysics, University of Chile.

Reanalysis data provided by the NOAA-CIRES Climate Diagnostics Center, Boulder, Colorado, USA, from their Web site at <http://www.cdc.noaa.gov/>

Part of the funding for this project came out of the budget of Onsala Space Observatory provided by the Swedish Natural Science Council (NFR).

References

- [1] S. Radford y M. Holdaway, “*Atmospheric Conditions at a Site for Submillimeter Wavelength Astronomy*”, in *Advanced Technology MMW, Radio, and Terahertz Telescopes*, T. Phillips ed., SPIE 3357, pp. 486-494, 1998.
- [2] <http://www.cdc.noaa.gov/>
- [3] E. Kalnay, M. Kanamitsu, R. Kistler, W. Collins, D. Deaven, L. Gandin, M. Iredell, S. Saha, G. White, J. Woollen, Y. Zhu, A. Leetmaa, R. Reynolds M. Chelliah, W. Ebisuzaki, W. Higgins, J. Janowiak, K. C. Mo, C. Ropelewski, J. Wang, Roy Jenne, and Dennis Joseph, “The NCEP/NCAR 40-Year Reanalysis Project”, *Bulletin of the American Meteorological Society*, Vol. No. 77, pp. 437-471, 1996.
- [4] http://www.cpc.noaa.gov/products/analysis_monitoring/cdus/prcp_temp_tables/library.txt
- [5] R. Bustos, “A 52-Year Climatological Study for the Chajnantor Area Using NCEP/NCAR Reanalysis Data of Pressure, Temperature, Specific Humidity and Precipitable Water,” Internal Report, European Southern Observatory, ALMA Project, 2000.
- [6] Kistler, R., E. Kalnay, W. Collins, S. Saha, G. White, J. Woollen, M. Chelliah, W. Ebisuzaki, M. Kanamitsu, V. Kousky, H. van den Dool, R. Jenne, and M. Fiorino, “The NCEP/NCAR 50-Year Reanalysis”, submitted to the *Bulletin of the American Meteorological Society*, June, 2000.
- [7] A. Thompson, J. Moran, and G. Swenson, *Interferometry and Synthesis in Radio Astronomy*, Krieger Publishing Company, 1994.
- [8] G. Delgado, A. Otárola, R. Booth, V. Belitsky, D. Urbain, R. Hills, and Y. Robson, “Phase Correlation of Interferometer Data at Mauna Kea and Chajnantor,” to be submitted to the ALMA Memo Series, 2000.
- [9] M. Salby, *Fundamentals of Atmospheric Physics*, Academic Press, San Diego, 1996.
- [10] J. T. Houghton, *The Physics of Atmospheres*, Cambridge University Press, 1986.
- [11] G. Delgado, A. Otárola, V. Belitsky, D. Urbain, and P. Martin-Cocher, “The Determination of Precipitable Water Vapour at Llano de Chajnantor from Observations of the 183 GHz Water Vapour Line,” ALMA Memo Series No. 271, 1999.
- [12] <http://www.tuc.nrao.edu/mma/sites/Chajnantor/data.c.html>
- [13] M. McKinnon, “Measurement of Atmospheric Opacity due to Water Vapor at 225 GHz,” ALMA Memo Series No. 40, 1987.
- [14] J. Hnilo, B. Santer, J. Boyle, K. Taylor, and C. Doutriaux, “Research Activities at the Program for Climate Model Diagnosis and Intercomparison,” in *Program for Climate Model Diagnosis and Intercomparison*, The Second International Conference on Reanalysis Reading, UK, August 1999.
- [15] R. Higgins, Y. Yao, M. Chelliah, W. Ebisuzaki, J. Janowiak, C. Ropelewski and R. Kistler, “Intercomparison of the NCEP/NCAR and the NASA/DAO Reanalyses (1985-1993),” NCEP/Climate Prediction Center, ATLAS No. 2, http://yao.wwb.noaa.gov:2000/atlas_2/toc_1.html
- [16] P. Aceituno, A. Montecinos, “Diurnal cycle over the South American altiplano: comparison of NCEP/NCAR reanalysis with upper-air observations during the Visviri field experiment,” published on the Proceedings of the *VI International Conference on Southern Hemisphere Meteorology and Oceanography*, pp. 4-28, 2000.
- [17] R. Bustos, “A 5-Year Cross-correlation Analysis of NCEP/NCAR Reanalysis Data with Chajnantor Ground Stations,” Internal Report, European Southern Observatory, ALMA Project, 2000.
- [18] K. Wolter, “Multivariate ENSO Index (MEI),” posted at the Climate Diagnostics Center web pages, <http://www.cdc.noaa.gov/%7Ekew/MEI/#outlook>
- [19] http://www.cpc.noaa.gov/products/analysis_monitoring/ensostuff/ensoyears.html

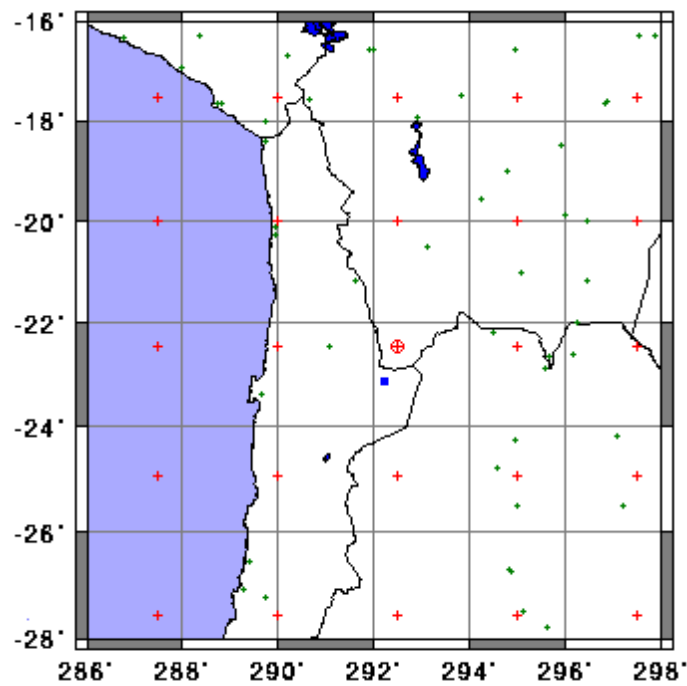


Fig.1. Ground stations are shown as green dots on the map. Red crosses are grid points for reanalysis output files. Central red circle corresponds to the closest grid point to the Chajnantor site (shown as a blue square).

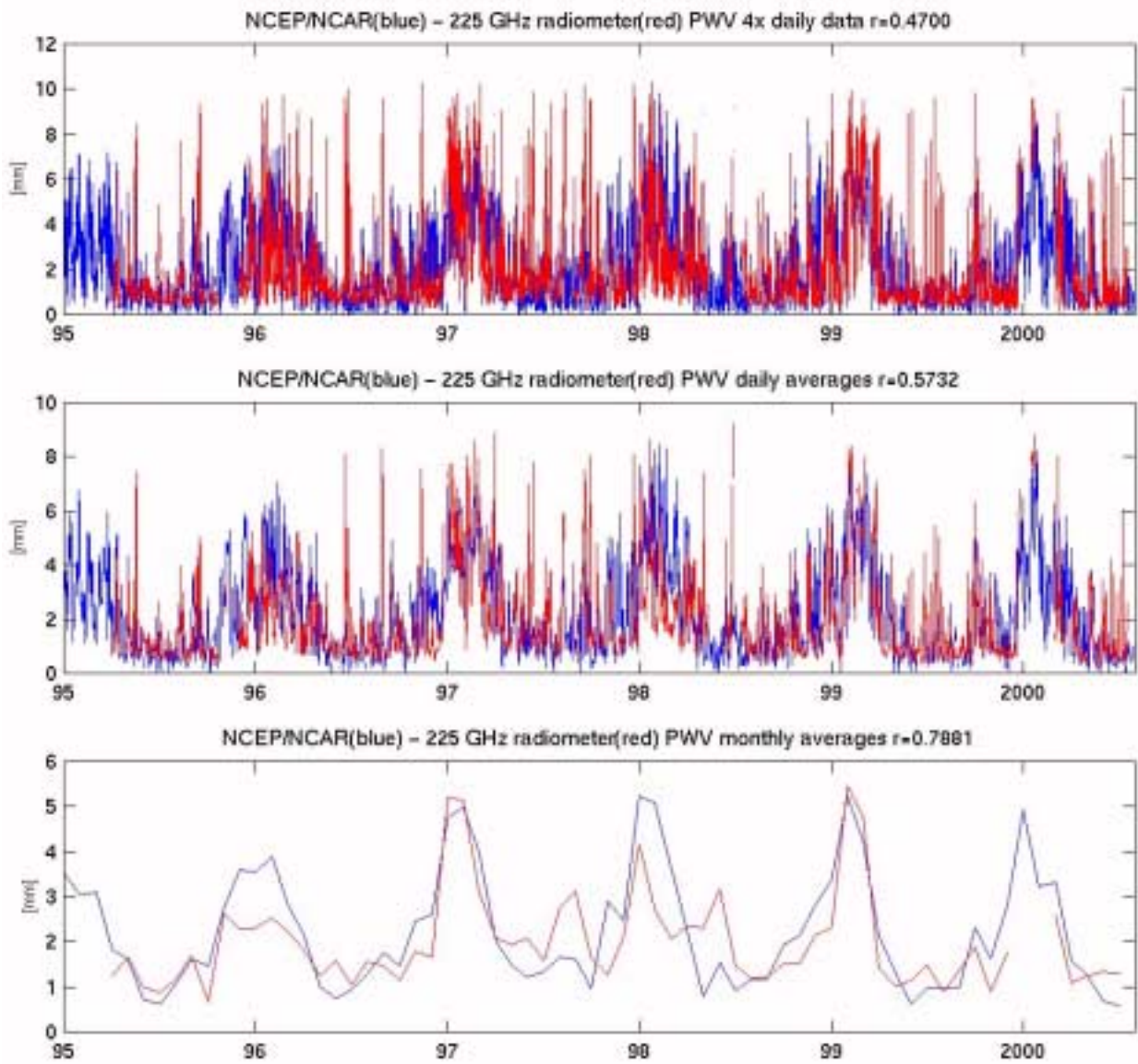


Figure 2. NCEP/NCAR data (blue solid line) and radiometer data (red solid line). The upper graph corresponds to four times per day measurements (00:00, 06:00, 12:00, and 18:00 UTC), the centre graph shows daily averages, and the bottom graph shows monthly averages. Negative NCEP/NCAR PWV values and opacity data greater than the equivalent of 10.4 mm of PWV have been eliminated.

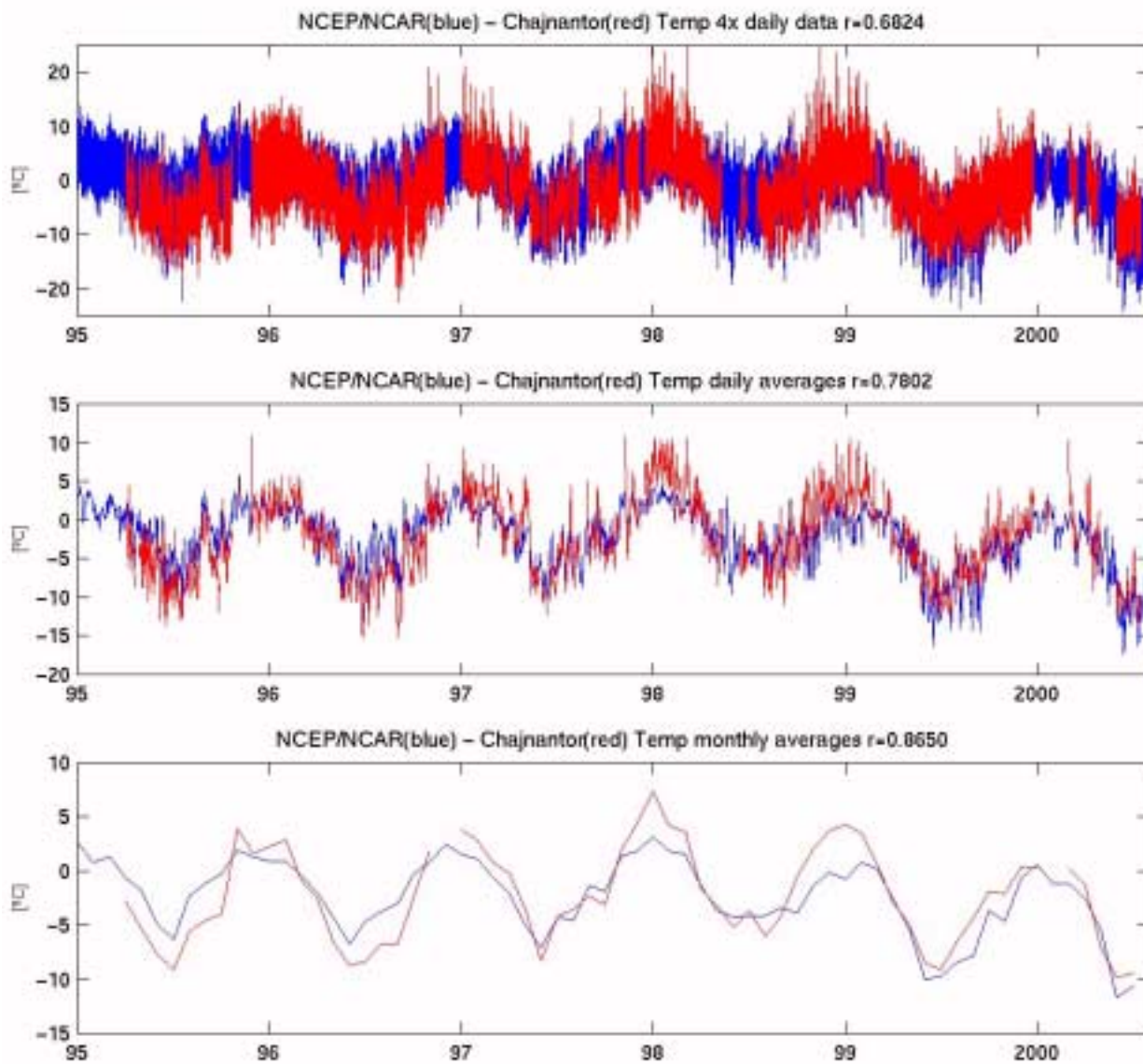


Figure 3. NCEP/NCAR temperature data (blue solid line) and Chajnantor ground-based temperature data (red solid line). The upper graph corresponds to four times per day measurements (00:00, 06:00, 12:00, and 18:00 UTC), the centre graph shows daily averages, and the bottom graph shows monthly averages. A constant 6.4°C has been subtracted from the NCEP/NCAR reanalysis temperature data in all graphs.

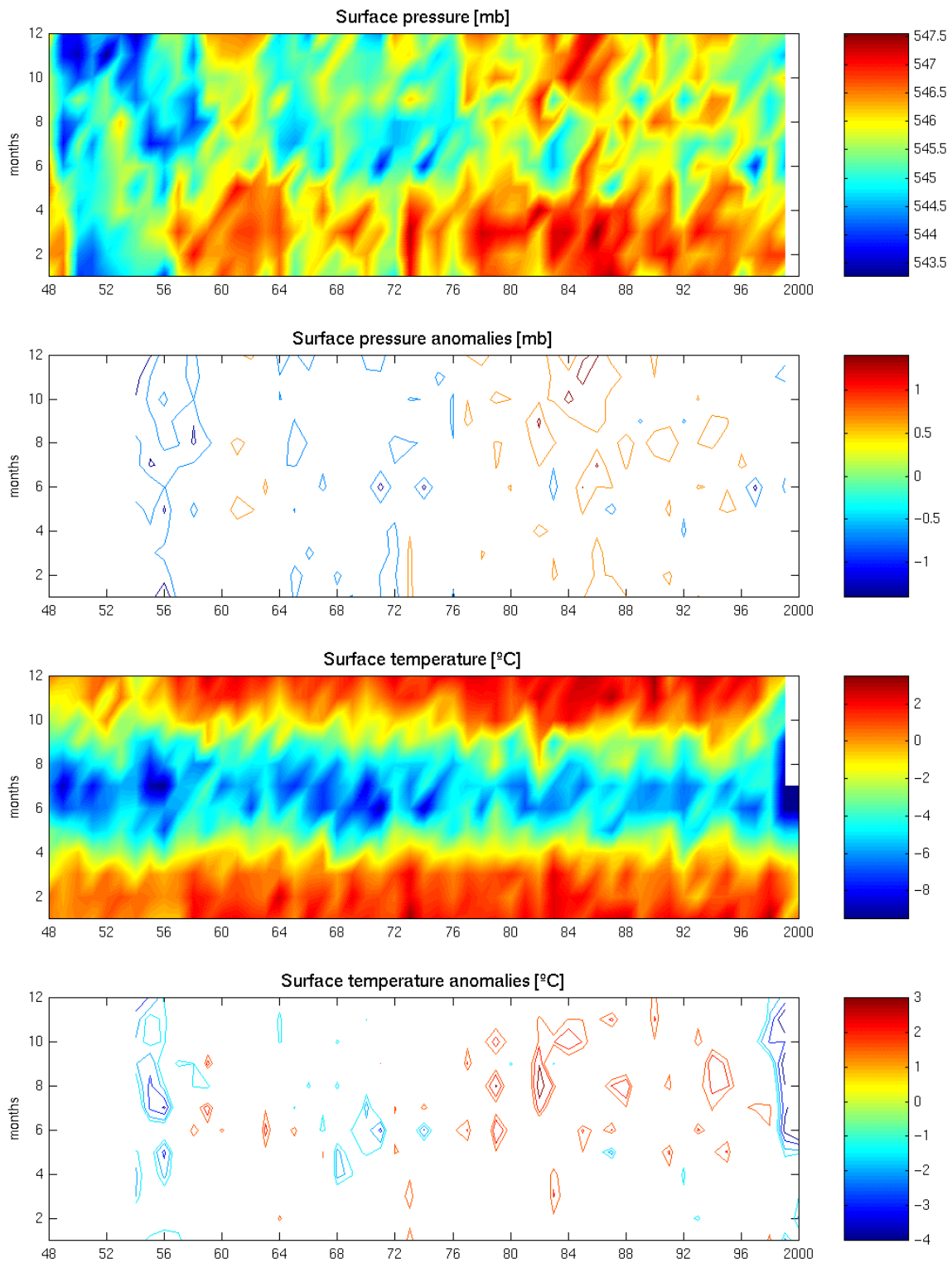


Figure 4. NCEP/NCAR surface data corrected for the altitude of Chajnantor. Upper two plots show the pressure, and the lower two plots show the temperature. The upper plot of each group corresponds to coloured isopleth diagrams (annually versus monthly values), the lower plot of each group shows contour lines for the anomalies of these variables as compared with the historical mean.

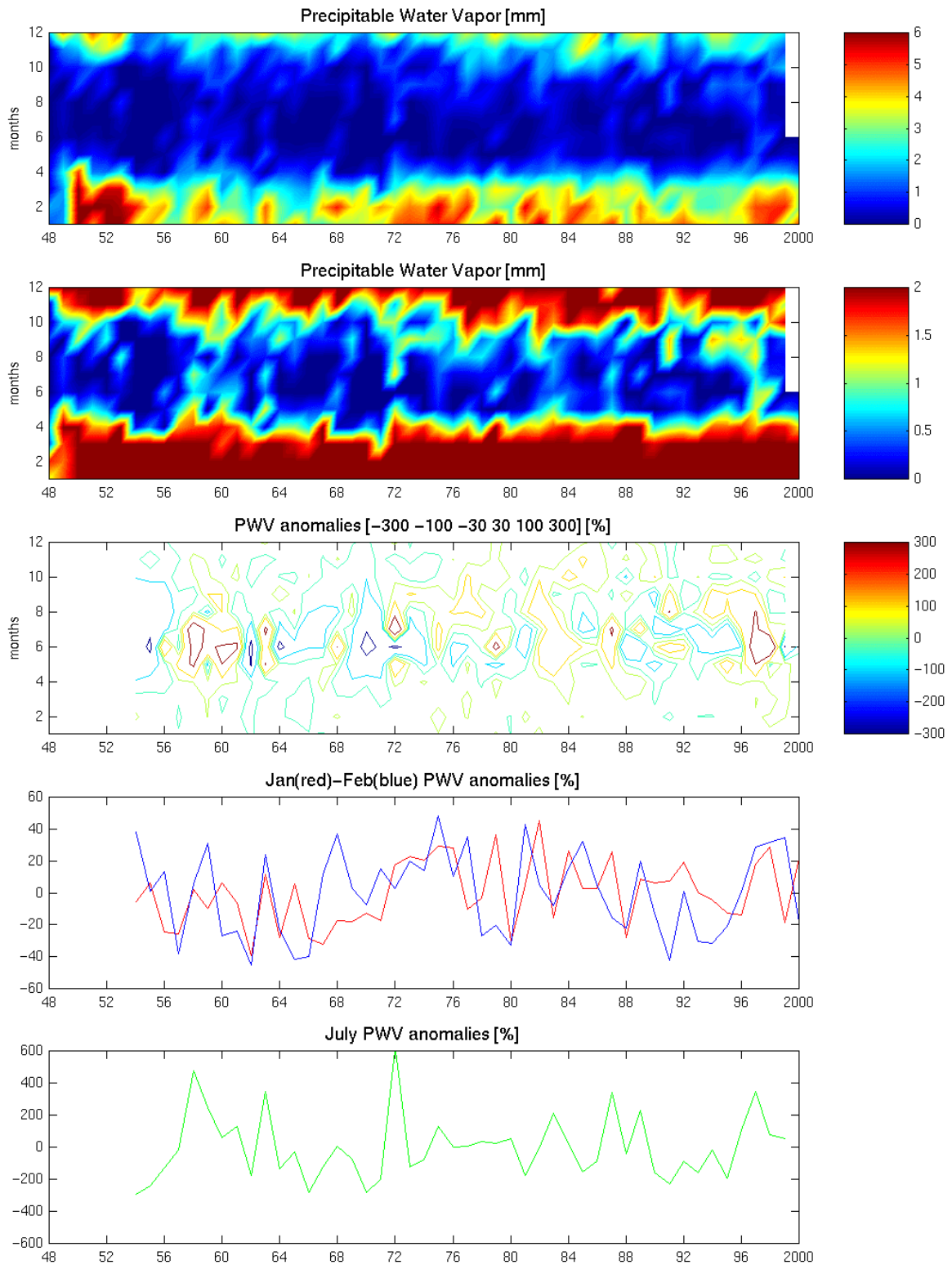


Figure 5. NCEP/NCAR surface *PWV* data corrected for the altitude of Chajnantor. Upper plot shows a coloured isopleth diagrams (annually versus monthly values) with low resolution (0-6 mm of *PWV*), while the second plot shows a higher resolution (0-2 mm of *PWV*). The centre plot shows anomalies in percentage. The fourth plot shows the anomalies in percentage for January and February (the summer storms months), and the lower plot shows the anomalies in percentage for the month of July (midst of austral winter).

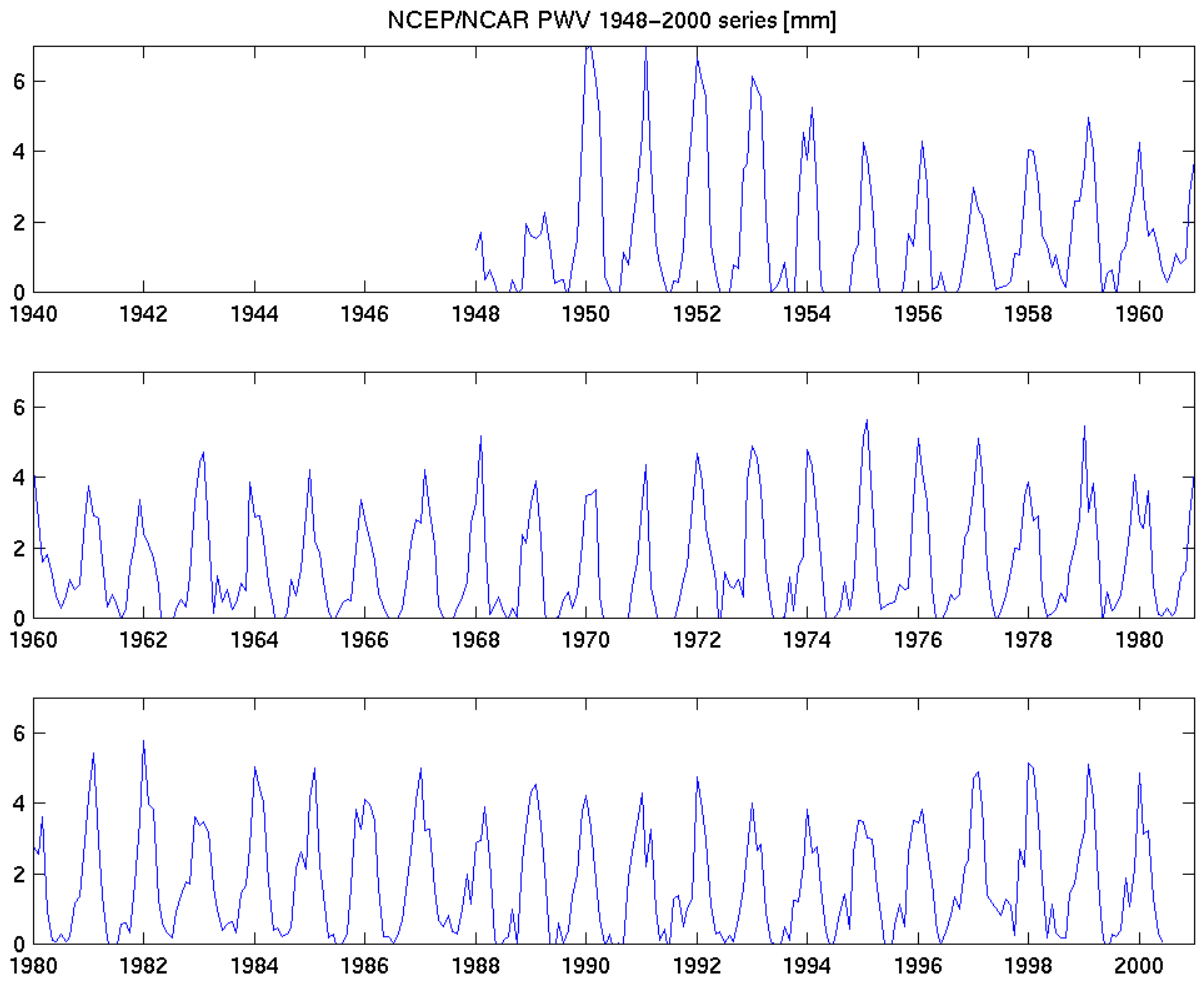


Figure 6. NCEP/NCAR reanalysis time series for *PWV* from 1948 to July 2000.

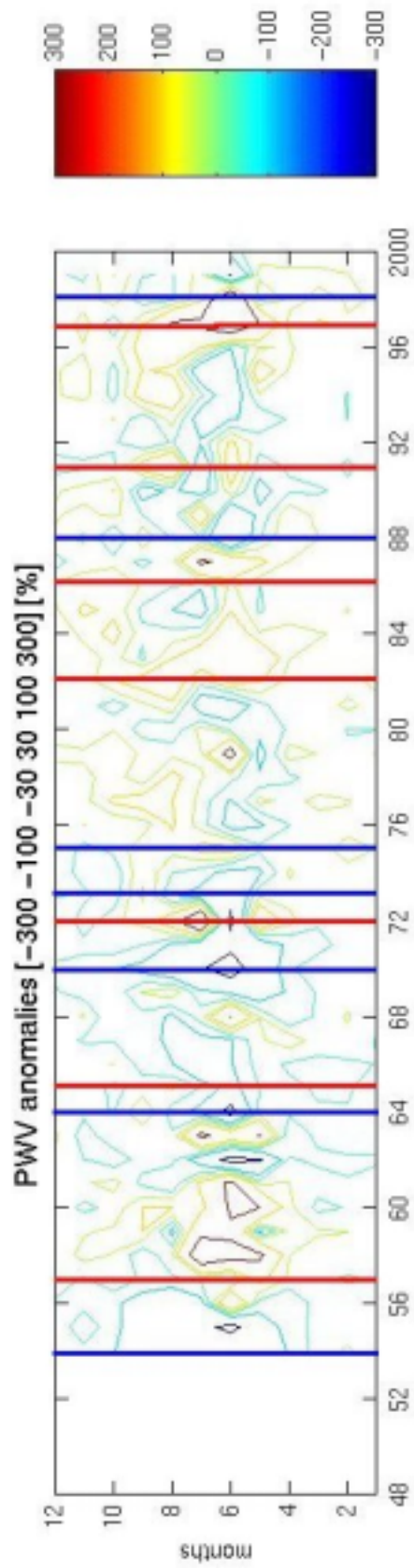


Figure 7. *PWV* anomalies from 1948 to July 2000 with the beginning of the strongest El Niño (red line) and La Niña events (blue line).